Electrical Detection of Domain Walls and Skyrmions in Co Films Using Noncollinear Magnetoresistance

Marco Perini,[1] Sebastian Meyer,[2] André Kubetzka,[1] Roland Wiesendanger,[1] Stefan Heinze,[2,*] and Kirsten von Bergmann[1]

[1]*Department of Physics, University of Hamburg, 20355 Hamburg, Germany*

[2]*Institute of Theoretical Physics and Astrophysics, University of Kiel, Leibnizstrasse 15, 24098 Kiel, Germany*

(Received 10 July 2019; revised manuscript received 14 October 2019; published 3 December 2019)

A large noncollinear magnetoresistance (NCMR) is observed for Rh/Co atomic bilayers on Ir(111) using scanning tunneling microscopy and spectroscopy. The effect is 20% at the Fermi energy and large in a broad energy range. The NCMR can be used to electrically detect nanometer-scale domain walls and skyrmions directly in the tunnel current without the need for a differential measurement. The NCMR results from changes in the density of states of noncollinear spin textures with respect to the ferromagnetic state. Density functional theory calculations reveal that they originate from spin mixing between majority d_{xz} and minority p_z states.

DOI: 10.1103/PhysRevLett.123.237205

It has been proposed to use localized, stable spin structures on a nanometer scale—such as domain walls (DWs) or skyrmions—in future magnetic memory or logic applications [1–4]. Key steps towards realizing such device concepts are the controlled writing and deleting of single nanoscale magnetic entities as well as the readout of the magnetic information. In planar magnetic tunnel junctions DWs have been detected via magnetoresistance effects [5,6]; however, despite several theoretical predictions [7,8], the detection of skyrmions has so far been reported only once [9]. In terms of simplified device fabrication and integration into present technologies all-electrical readout schemes of magnetic bits [10] are beneficial. The anomalous Hall effect allows such electrical detection of DWs [11] as well as skyrmions [12,13]; however, for such lateral transport measurements a Hall bar junction needs to be integrated into the device structure.

An alternative route is to exploit the recently discovered noncollinear magnetoresistance (NCMR) [14] which has been observed in scanning tunneling microscopy (STM) experiments and allows all-electrical detection of skyrmions [14–16]. This effect occurs due to spin mixing of the two spin channels in a noncollinear spin structure [14,17]. Therefore, it is typically much larger than the tunneling anisotropic magnetoresistance [18,19], which stems from spin-orbit coupling. However, so far the NCMR has only been reported for skyrmions in two different Fe-based films and only at bias voltages a few 100 meV away from the Fermi energy [14–16], which is not well suited for potential device applications in planar tunnel junctions.

Here, we report the observation of a large NCMR in Rh/Co atomic bilayers on Ir(111) in a broad energy range, with about 20% at the Fermi energy. This allows for an easy detection of nanometer thin DWs as well as sub-5 nm magnetic skyrmions using scanning tunneling microscopy (STM). The observed NCMR can be explained based on density functional theory (DFT) calculations of the electronic structure of the Rh/Co films. The NCMR stems from spin mixing of majority d_{xz} and minority p_z states and it can be well described within a simplified tight-binding model. We find that the contribution from spin-orbit coupling is small in comparison.

Figure 1(a) shows an overview image of a sample of Rh/Co/Ir(111) [20], where the constant-current topography is colorized with the spin-resolved differential conductance dI/dU. The submonolayer amount of Co grows in step-flow growth mode from the step edges of the Ir(111) single crystal surface. The subsequently deposited Rh forms monolayer high islands of both stackings on the Co stripes and directly on the bare Ir surface (see Ref. [21]). Here, we will focus on the hcp-stacked Rh on the Co monolayer, which can be identified in Fig. 1(a) by the blue color. The two different shades of blue originate from the tunneling magnetoresistance (TMR) effect and represent the two oppositely magnetized out-of-plane ferromagnetic (FM) orientations. The brighter lines separating two FM domains are the DWs, which show a higher dI/dU signal compared to that of the FM domains due to the NCMR of this Rh/Co atomic bilayer [20]. A circular DW, representing a magnetic skyrmion with a diameter of about 3 nm, is indicated by the red circle [20].

The dI/dU map of Fig. 1(b) was obtained with a spin-averaging tip and now the DWs, visible as brighter lines, separate domains that do not exhibit a magnetic contrast. When the tip is modified by gentle tip-sample collisions it can become spin polarized, and the dI/dU map of Fig. 1(c)

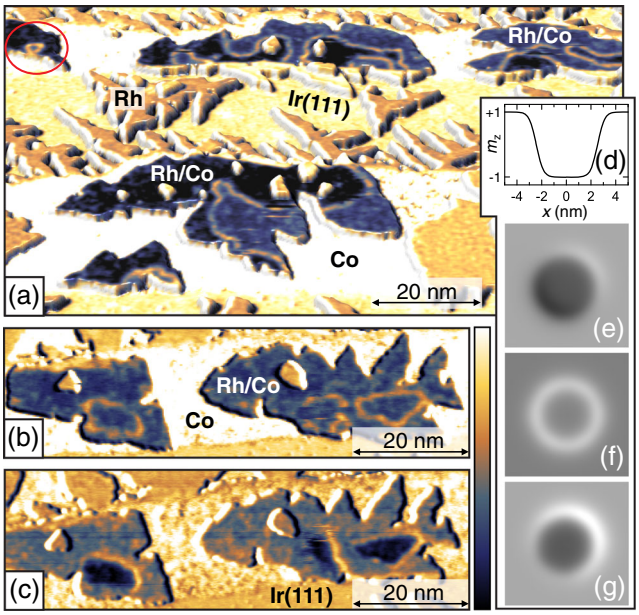

FIG. 1. (a) Constant-current STM image colorized with the spin-resolved dI/dU signal of a sample of about 0.4 atomic layers of Rh on 0.6 atomic layers of Co on Ir(111). The hcp-stacked Rh islands can be identified by their blue color, thin lines indicate DWs between oppositely oriented out-of-plane FM domains. The red circle highlights a skyrmion observed in the hcp-Rh/Co atomic bilayer. The corresponding color bar is shown below. (b) and (c) dI/dU maps of identical sample areas imaged with spin-averaging and spin-resolving tip, respectively; the bright roughly triangular-shaped objects on the hcp-Rh/Co are small islands of Rh on top of the film. Images (a)–(c) were taken at $T = 4.2$ K, $U = -250$ mV, and $I = 0.8$ nA with a Cr bulk tip. (d) Line profile across a modeled magnetic skyrmion with a diameter of 5 nm and corresponding STM simulations of (e) the TMR signal with a canted tip magnetization, (f) the NCMR signal, and (g) a combination of both.

was obtained with such a spin-sensitive tip, now giving rise to a two-stage TMR contrast for the oppositely magnetized FM domains. There is also a variation of the dI/dU signal on the DWs, meaning that the tip magnetization is canted and thus sensitive to both out-of-plane as well as in-plane magnetization components. We find that all three darker domains show a higher TMR signal on the DW to the right side, which demonstrates that all three magnetic structures have the same sense of magnetization rotation caused by the interfacial Dzyaloshinskii-Moriya interaction (DMI); in thin-film systems it favors Néel-type DWs and skyrmions with unique rotational sense.

We illustrate the details of the observed dI/dU contrasts by STM simulations [14,26] (see Ref. [21]) of an individual skyrmion, see skyrmion profile in Fig. 1(d), using different contributions for the TMR and the NCMR signal. An STM simulation using only TMR with a canted tip magnetization direction is shown in (e): in this example the core of the skyrmion is darker than the surrounding FM background, and the DW is brighter on the upper right side of the skyrmion and darker on the lower left side. We model the NCMR as proportional to the average angle between a spin and its nearest neighbor spins. When only NCMR is considered in the STM simulations a bright ring is observed, Fig. 1(f), in agreement with the data in Fig. 1(b) obtained with a spin-averaging tip. To reproduce the features of the dI/dU map shown in Fig. 1(c) both TMR and NCMR contributions need to be included in the STM simulation, see Fig. 1(g).

In order to reveal the origin of the electronic NCMR contrast which allows an all-electrical detection of DWs and skyrmions we performed dI/dU spectroscopy and compare it with DFT calculations. The DFT calculations were carried out using the FLEUR code [27] which is based on the full-potential linearized augmented plane wave method. Computational details can be found in Ref. [21]. Figure 2(a) shows a spin-polarized dI/dU map of Rh/Co with three FM domains separated by two DWs. The spin-averaged spectra for FM domains and DWs displayed in Fig. 2(b) were obtained by averaging the two spectra on oppositely magnetized FM domains, and DWs, respectively [see colored dots in Fig. 2(a)]. The two peaks found in the dI/dU spectra show different intensities and energies for the FM domain compared to the DW. The magnetoresistance (MR), defined as

$$\mathrm{MR} = \frac{dI/dU_{\mathrm{FM}} - dI/dU_{\mathrm{DW}}}{dI/dU_{\mathrm{FM}}} \tag{1}$$

is shown in Fig. 2(c) as a function of the sample bias voltage. We find that the NCMR is large in a broad energy window. It is around 20% at the Fermi energy, which implies that DWs and skyrmions can also be detected in transport measurements with planar tunnel junctions, as anticipated for applications.

Within the Tersoff-Hamann model the dI/dU signal is proportional to the local density of states (LDOS) in the vacuum a few Å above the surface [28]. We locally approximate the spin structure within the DW by a homogeneous spin spiral which can be calculated via DFT [23]. Figure 2(d) shows the vacuum LDOS of Rh/Co/Ir(111) obtained via DFT for the FM state and for homogeneous spin spirals propagating along the direction of nearest neighbors ($\bar{\Gamma} - \bar{K}$ direction) with varying angle θ between neighboring spins [see inset of Fig. 2(d)]. The changes of the electronic structure originate from the noncollinearity of the spin texture [29]. In the FM state there is a pronounced vacuum LDOS peak just above the Fermi energy, E_F, and a smaller peak about 0.2 eV lower in energy. This peak structure is similar to that found in the experimental dI/dU spectrum of the FM domains.

As the angle in the spin spiral increases, the peak near the Fermi energy shifts to higher energies and drops in height. This behavior is roughly linear in θ [Fig. 2(f)] as in Pd/Fe/Ir(111) [14]. For an angle of $\theta = 16.4°$ the peak shift and height drop are in good agreement with the

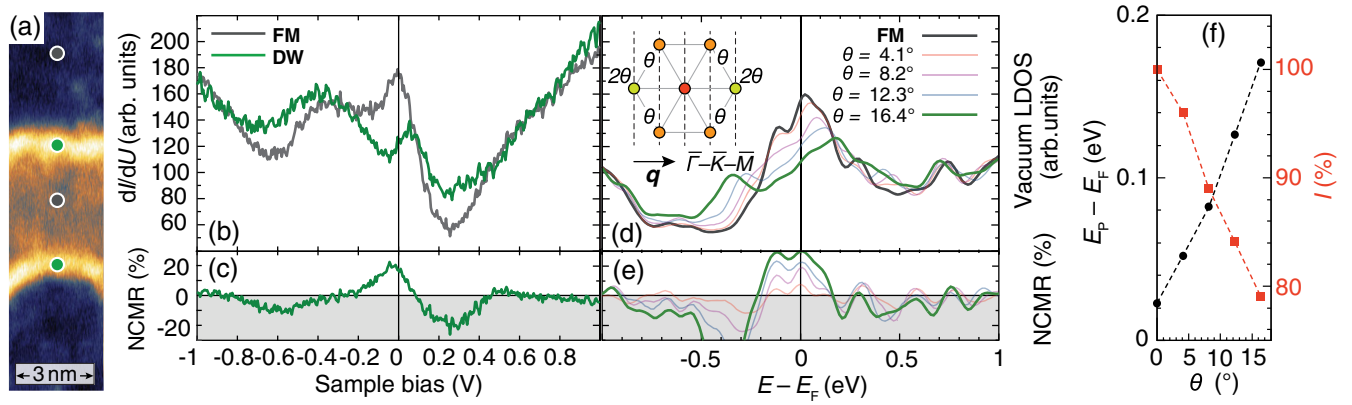

FIG. 2. (a) Spin-resolved dI/dU map of Rh/Co/Ir(111) with three FM domains separated by two DWs measured at −250 mV. (b) Spin-averaged dI/dU spectra obtained by averaging the spectra taken at the color-coded points in (a), feedback switched off at −1 V and 1 nA; see also Ref. [21]. (c) NCMR calculated according to Eq. (1) using the two spectra in (b). (d) Calculated vacuum LDOS 3 Å above the film of Rh/Co/Ir(111) for the FM state (gray curve) and for spin spirals with different nearest-neighbor angles θ (colored curves). The zero line is aligned with that in (b). The inset shows a sketch of the hexagonal atomic lattice with the spin spiral propagation direction given by $\mathbf{q}$ and the angle θ between spins on neighboring sites. (e) NCMR calculated from the FM and spin spiral vacuum LDOS for different θ. (f) Peak position (E_P) relative to E_F (black points) and peak intensity relative to the main peak of the FM state at $E_F + 0.04$ eV (red points) for the calculated spin spiral curves as a function of θ.

experimental observation between the FM domain and DW. This angle corresponds reasonably well to the maximum nearest neighbor angle of about 19° obtained for the center of a DW with a width of about 0.8 nm (see Ref. [20] for experimental DW profiles).

The theoretical MR shown in Fig. 2(e) is obtained by using the energy-dependent vacuum LDOS in the FM and the spin spiral state instead of the dI/dU signal. As in the experiments it is large in a broad energy regime including the Fermi energy [30].

We have checked the contribution of spin-orbit coupling (not taken into account in the spin spiral calculations) to the magnetoresistance by calculating the vacuum LDOS for a FM film with a magnetization direction in the film plane and perpendicular to the film. The changes in this tunneling anisotropic magnetoresistance are below 5% and vary on a much smaller energy scale (see Ref. [21]). Therefore, we conclude that the experimentally observed electronic effect is dominantly due to spin mixing, i.e., the NCMR.

Deeper insight into the origin of the NCMR effect can be obtained by taking a look at the LDOS within the surface layer, see Fig. 3(a). Because of hybridization with the Co layer the LDOS of the Rh atoms is spin polarized and the Rh atoms exhibit a magnetic moment of about $0.6\mu_B$ in the FM state. From an analysis of the Rh LDOS we find that the characteristic double peak structure in the vacuum LDOS around E_F stems from minority p_z orbitals which decay slowly into the vacuum as they are pointing out of the surface; the majority d_{xz} states only have a minor contribution to the vacuum LDOS.

Upon rotation of the spin direction of adjacent magnetic moments within the Rh/Co bilayer the minority p_z peak slightly above E_F moves to higher energies and is reduced in peak height. The peak below E_F also slowly diminishes with increasing angle and an additional peak appears at an energy of about 0.3 eV below E_F. This modification of the LDOS of the minority p_z state is directly reflected in the vacuum LDOS [cf. Fig. 2(d)]. The majority spin counterpart for the spin mixing is a d_{xz} state located at $E_F - 0.25$ eV [Fig. 3(a) top], which, accordingly, also changes and shows a peak shift to lower energies along with decreasing peak height with increasing rotation angle θ. The spin mixing in the adjacent Co layer involves similar states (see Ref. [21]).

The effect of spin mixing between the two states can be understood within a simplified tight-binding model that can be solved analytically. We consider two states located at energies $\epsilon_\uparrow$ and $\epsilon_\downarrow$ in the majority and minority spin channel, respectively. The hopping between the two states $t(\theta)$ depends on the angle θ between the spin quantization axes of adjacent atoms within the film according to the spin rotation matrices, i.e., $t(\theta) = t_0 \sin\theta/2$. The Hamiltonian of this model is given by

$$H = \begin{pmatrix} \epsilon_\uparrow & -t(\theta) \\ -t(\theta) & \epsilon_\downarrow \end{pmatrix}. \tag{2}$$

Because of hybridization with the neighboring atoms the states are broadened with a full width at half maximum of $\gamma_{\uparrow,\downarrow}$, which is incorporated into the model by the self-energy Σ given by

$$\Sigma = \begin{pmatrix} -i\gamma_\uparrow & 0 \\ 0 & -i\gamma_\downarrow \end{pmatrix} \tag{3}$$

and the Green's function $G(E)$ can be determined from the equation $(E\mathbb{I} - H - \Sigma)G(E) = \mathbb{I}$, which yields the LDOS

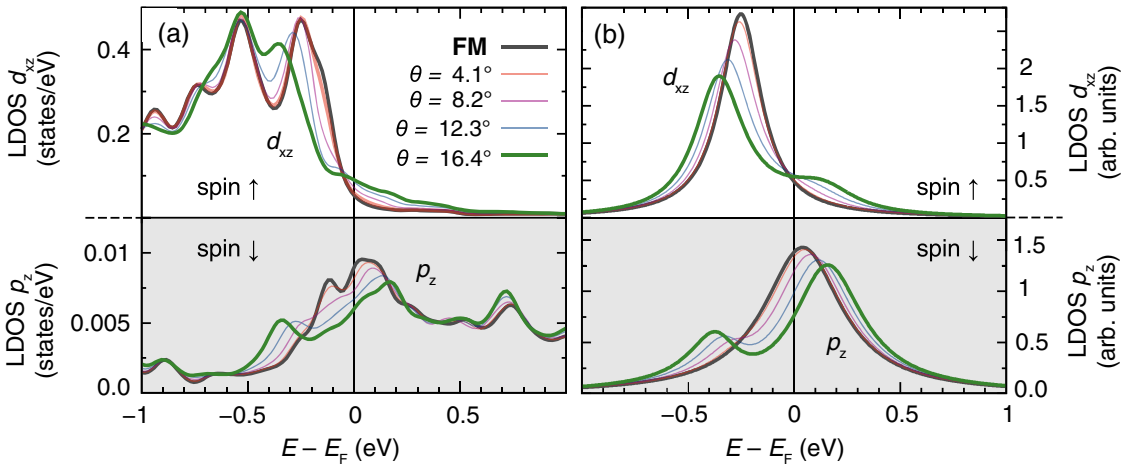

FIG. 3. Orbital and spin decomposition of the local density of states (LDOS) at the Rh atom. (a) LDOS of the majority d_{xz} (upper panel) and minority p_z states (lower panel) obtained from DFT calculations for spin spiral states with an angle θ between adjacent spins as given in the legend. (b) LDOS of the states obtained within a simplified two-state tight-binding model (see text for details).

in the two spin channels from the diagonal elements of the Green's function: $n_\sigma(E) = -(1/\pi)\mathrm{Im}[G_{\sigma\sigma}(E)]$.

We obtain the model parameters by fitting Lorentzian curves to the majority d_{xz} state and the minority p_z state, which yields $\epsilon_\uparrow = E_F - 0.25$ eV, $\gamma_\uparrow \approx 0.12$ eV and $\epsilon_\downarrow = E_F + 0.04$ eV, $\gamma_\downarrow \approx 0.22$ eV, respectively. The hopping matrix element $t_0 = 1.5$ eV is fixed such that the shift of the p_z state at an angle of $\theta = 16.4°$ agrees with that from the DFT calculation.

The LDOS obtained from this model for the FM state, i.e., without spin mixing and a vanishing nondiagonal part of the Hamiltonian, is displayed in Fig. 3(b) as gray lines for the two spin channels. Upon increasing θ the hopping term rises and spin mixing between the two states occurs. Because of this hybridization the peak of the minority p_z state moves to higher energies and its intensity drops, which leads to the characteristic behavior seen in Fig. 2(f). The majority d_{xz} state moves to lower energies and decreases. The similarities with the full DFT calculation show that the simplified model already captures the essential physics of the spin mixing [31].

In conclusion, we have observed a large noncollinear magnetoresistance (NCMR) of 20% at the Fermi energy in ultrathin Rh/Co films, enabling the detection of nanoscale domain walls and skyrmions in tunnel junctions with a nonmagnetic electrode. The origin of this effect stems from spin mixing between p and d states as shown based on first-principles calculations. This demonstrates that the NCMR is not limited to Fe-based materials but that it is a general phenomenon and consequently also occurs in Co-based films. Because the states involved in the spin mixing are close to the Fermi energy, the NCMR is large at zero bias, highlighting its potential as an all-electrical readout concept for spintronic applications to detect localized spin textures such as domain walls and skyrmions.

This work was funded by the European Union's Horizon 2020 research and innovation programme under Grant Agreement No. 665095 (FET-Open project MAGicSky). S. M. and S. H. gratefully acknowledge computing time at the supercomputer of the North-German Supercomputing Alliance (HLRN). K. v.B. and A. K. acknowledge financial support from the Deutsche Forschungsgemeinschaft (DFG, German Research Foundation)—402843438;—408119516.

*Corresponding author.
heinze@physik.uni-kiel.de

[1] S. S. P. Parkin, M. Hayashi, and L. Thomas, Science **320**, 190 (2008).
[2] A. Fert, V. Cros, and J. Sampaio, Nat. Nanotechnol. **8**, 152 (2013).
[3] R. Wiesendanger, Nat. Rev. Mater. **1**, 16044 (2016).
[4] A. Fert, N. Reyren, and V. Cros, Nat. Rev. Mater. **2**, 17031 (2017).
[5] K. Kondou, N. Ohshima, S. Kasai, Y. Nakatani, and T. Ono, Appl. Phys. Express **1**, 061302 (2008).
[6] A. Chanthbouala, R. Matsumoto, J. Grollier, V. Cros, A. Anane, A. Fert, A. V. Khvalkovskiy, K. A. Zvezdin, K. Nishimura, Y. Nagamine, H. Maehara, K. Tsunekawa, A. Fukushima, and S. Yuasa, Nat. Phys. **7**, 626 (2011).
[7] K. Hamamoto and N. Nagaosa, arxiv:1803.04588.
[8] J. F. Schäfer, P. Risius, M. Czerner, and C. Heiliger, arxiv:1901.10313.
[9] N. E. Penthorn, X. Hao, Z. Wang, Y. Huai, and H. W. Jiang, Phys. Rev. Lett. **122**, 257201 (2019).
[10] T. L. Monchesky, Nat. Nanotechnol. **10**, 1008 (2015).
[11] S. F. Zhang, W. L. Gan, J. Kwon, F. L. Luo, G. J. Lim, J. B. Wang, and W. S. Lew, Sci. Rep. **6**, 24804 (2016).
[12] D. Maccariello, W. Legrand, N. Reyren, K. Garcia, K. Bouzehouane, S. Collin, V. Cros, and A. Fert, Nat. Nanotechnol. **13**, 233 (2018).

[13] K. Zeissler, S. Finizio, K. Shahbazi, J. Massey, F. Al Ma'Mari, D. M. Bracher, A. Kleibert, M. C. Rosamond, E. H. Linfield, T. A. Moore, J. Raabe, G. Burnell, and C. H. Marrows, Nat. Nanotechnol. **13**, 1161 (2018).
[14] C. Hanneken, F. Otte, A. Kubetzka, B. Dupé, N. Romming, K. von Bergmann, R. Wiesendanger, and S. Heinze, Nat. Nanotechnol. **10**, 1039 (2015).
[15] A. Kubetzka, C. Hanneken, R. Wiesendanger, and K. von Bergmann, Phys. Rev. B **95**, 104433 (2017).
[16] P.-J. Hsu, A. Kubetzka, A. Finco, N. Romming, K. von Bergmann, and R. Wiesendanger, Nat. Nanotechnol. **12**, 123 (2017).
[17] D. M. Crum, M. Bouhassoune, J. Bouaziz, B. Schweflinghaus, S. Blügel, and S. Lounis, Nat. Commun. **6**, 8541 (2015).
[18] M. Bode, S. Heinze, A. Kubetzka, O. Pietzsch, X. Nie, G. Bihlmayer, S. Blügel, and R. Wiesendanger, Phys. Rev. Lett. **89**, 237205 (2002).
[19] C. Gould, C. Rüster, T. Jungwirth, E. Girgis, G. M. Schott, R. Giraud, K. Brunner, G. Schmidt, and L. W. Molenkamp, Phys. Rev. Lett. **93**, 117203 (2004).
[20] S. Meyer, M. Perini, S. von Malottki, A. Kubetzka, R. Wiesendanger, K. von Bergmann, and S. Heinze, Nat. Commun. **10**, 3823 (2019).
[21] See Supplemental Material at http://link.aps.org/supplemental/10.1103/PhysRevLett.123.237205 for experimental and computational details and notes on the quantitative comparison of dI/dU spectra and LDOS, which includes Refs. [22–25].
[22] N. Romming, A. Kubetzka, C. Hanneken, K. von Bergmann, and R. Wiesendanger, Phys. Rev. Lett. **114**, 177203 (2015).
[23] P. Kurz, F. Förster, L. Nordström, G. Bihlmayer, and S. Blügel, Phys. Rev. B **69**, 024415 (2004).
[24] L. M. Sandratskii, J. Phys. Condens. Matter **3**, 8565 (1991).
[25] S. H. Vosko, L. Wilk, and M. Nusair, Can. J. Phys. **58**, 1200 (1980).
[26] S. Heinze, Appl. Phys. A **85**, 407 (2006).
[27] www.flapw.de.
[28] J. Tersoff and D. R. Hamann, Phys. Rev. Lett. **50**, 1998 (1983).
[29] We have also calculated spin spirals along the other high symmetry direction of the Brillouin zone, i.e., $\bar{\Gamma}-\bar{M}$, and obtained qualitatively similar results as shown in Ref. [21].
[30] The possible origin of quantitative deviations between the LDOS and the dI/dU spectra are discussed in Ref. [21].
[31] Certainly, there are effects in the LDOS of the DFT calculation which are beyond the simplified model such as the second smaller p_z peak, which occurs at about $E_F - 0.1$ eV in the FM state [cf. Fig. 3(a)].